WPS1-CPR(18) 19203

A Langenberg et al.

Impurity Transport Studies at Wendelstein 7-X by Means of X-ray Imaging Spectrometer Measurements

Preprint of Paper to be submitted for publication in Proceeding of 45th European Physical Society Conference on Plasma Physics (EPS)

This work has been carried out within the framework of the EUROfusion Consortium and has received funding from the Euratom research and training programme 2014-2018 under grant agreement No 633053. The views and opinions expressed herein do not necessarily reflect those of the European Commission.

Impurity Transport Studies at Wendelstein 7-X by Means of X-ray Imaging Spectrometer Measurements[a)]

A. Langenberg,[1, b)] F. Warmer,[1] G. Fuchert,[1] A. Dinklage,[1] Th. Wegner,[1] J.A. Alonso,[2] S. Bozhenkov,[1] K.J. Brunner,[1] R. Burhenn,[1] B. Buttenschön,[1] P. Drews,[3] B. Geiger,[1] O. Grulke,[1, 4] M. Hirsch,[1] U. Höfel,[1] K.P. Hollfeld,[3] C. Killer,[1] J. Knauer,[1] T. Krings,[3] U. Neuner,[1] G. Offermanns,[3] N.A. Pablant,[5] E. Pasch,[1] K. Rahbarnia,[1] G. Satheeswaran,[3] J. Schilling,[1] B. Schweer,[3] H. Thomsen,[1] P. Traverso,[6] R.C. Wolf,[1] and the W7-X Team[c)]

[1)] *Max-Planck-Institut für Plasmaphysik, 17491 Greifswald, Germany*
[2)] *Laboratorio Nacional de Fusión, Asociación EURATOM-CIEMAT, Madrid, Spain*
[3)] *Forschungszentrum Jülich GmbH, Institut für Energie- und Klimaforschung - Plasmaphysik, 52425 Jülich, Germany*
[4)] *Technical University of Denmark DTU, Dept Phys, PPFE, DK-2800 Lyngby, Denmark*
[5)] *Princeton Plasma Physics Laboratory, Princeton, NJ, USA*
[6)] *Auburn University, Auburn, Alabama, USA*

(Dated: 2 July 2018)

This paper reports on the scaling of impurity transport properties with respect to a variation of heating power P_{ECRH} and electron density n_e for centrally electron cyclotron resonance heated He plasmas on the optimized stellarator Wendelstein 7-X. In a systematic P_{ECRH} - n_e scan, impurity transport times τ_I have been determined after Fe impurity injections by laser ablations and monitoring the temporal impurity emissivities by the x-ray imaging spectrometer HR-XIS. The observed τ_I scaling compares well to known τ_I scaling laws observed in other machines. A comparison of τ_I with the energy confinement times τ_E shows τ_E to be slightly enhanced with an averaged ratio of $\tau_E/\tau_I = 1.3$ and transport times in the range of τ_I=40-130 ms and τ_E=40-190 ms. A significant increase of τ_I has been observed when changing the power deposition from on- to off-axis heating with τ_E being mainly unaffected.

PACS numbers: Valid PACS appear here

I. INTRODUCTION

Due to non axis-symmetric 3D magnetic fields, impurity transport in the hot plasma core in stellarators is expected to be fundamentally different to tokamaks. In view of reactor-like operation, understanding the impurity transport is a prerequisite for steady-state operation. These aspects motivate initial impurity transport studies in W7-X at previously - in optimized stellarators – unexplored, reactor-relevant collisionalities. New effects, like potential variations on flux-surfaces[1] or screening effects due to species dependent transport regimes[2] are examples for aspects which attracted recent interest.
Experimentally, impurity transport investigations have been performed using several techniques, as *e.g.* monitoring the spatial and/or temporal emissivities of pulsed impurity injections[3–7] or intrinsic impurities[8,9]. From the experimental data, several transport relevant plasma parameters as the impurity transport time τ_I[10,11], the diffusive and convective transport parameters D and v[12–18] or the radial electric field E_r[19], can be determined either directly or from a comparison with transport code calculations.
As in many large scale fusion experiments, an empiric scaling of the impurity confinement with heating power P_{ECRH} and electron density n_e has been observed[3,6], in this work initial systematic P_{ECRH} - n_e scans have been performed at W7-X in Helium plasmas within two different magnetic configurations comparing measured impurity transport and energy confinement times. Furthermore, the impact of the specific settings of the heating power deposition on the impurity confinement has been investigated.

II. EXPERIMENTAL SETUP

For the investigation of impurity transport properties in W7-X, non recycling Fe impurities have been injected into the plasma using a Laser Blow-off (LBO) system[11]. After injection, the spatio-temporal evolution of impurities has been monitored using two X-ray imaging spectrometer systems, namely the X-ray Imaging Crystal Spectrometer (XICS) and the High Resolution X-ray Imaging Spectrometer (HR-XIS)[10,20]. The temporal evolution of the recorded brightness of selected impurity emission lines gives rise to impurity transport times τ_I, being a direct measure of global impurity transport properties[10].

[a)]Invited paper published as part of the Proceedings of the 45th Conference on Plasma Physics (EPS), Prague, Czech Republic, July, 2018.

[b)]andreas.langenberg@ipp.mpg.de
[c)]R.C. Wolf *et al.* Nuclear Fusion **57**, 102020 (2017).

A. Laser Blow-off System

The injection of non recycling, mainly metallic impurities such as Al, Ti, Fe, Mo, W, and Si is realized using the laser blow-off technology. Here, atoms, clusters, and macroscopic particles are ablated out of a 2-5 μm thick material layer covering a glass target by firing a laser onto the target. The laser used at W7-X is a Nd:YAG laser with 1 J laser energy and a maximum repetition rate of 20 Hz. It is guided onto the target holder via several mirrors with the last mirror being steerable allowing to adjust the laser spot position on the target. The glass target holder can mount up to 4 glass targets and is located 65 cm away from the last closed flux surface of the magnetic standard configuration EIM[21]. An observation camera installed behind the target holder allows an observation of the evaporation process. Depending on the target material, its thickness and the laser spot diameter, impurities in the order of 1×10^{18} particles can be evaporated per laser pulse. The detailed design and performance of the system has been described by Wegner *et al.*[11].

B. Imaging Spectrometers XICS and HR-XIS

The imaging spectrometers XICS and HR-XIS are equipped with several different crystals for the observation of the X-ray emission of various impurity species in highly ionized charge states. Making use of the imaging properties of a spherical bent crystal, X-rays emitted from the plasma impurities are imaged onto a two dimensional detector area, yielding energy and spatial resolution in horizontal and vertical direction on the detector. A spectral fit[22] and a tomographic inversion[12,23] of recorded spectra provides radial profiles of the impurity density $n_Z(\rho)$, ion and electron temperature, $T_i(\rho)$ and $T_e(\rho)$, and plasma rotation $v(\rho)$ with ρ defined as the square root of the magnetic flux ψ, normalized to the last closed flux surface: $\rho = \sqrt{(\psi/\psi_{LCFS})}$. For this study, the emission of He-like Fe (FeXXV) has been monitored with a Ge(422) crystal under a Bragg angle of 53.61° using the HR-XIS system. With a viewing geometry from the plasma center towards well above the mid plasma radius ($\rho = 0 - 0.6$) and a maximal time resolution of $t = 2$ ms, HR-XIS is well suited for transport investigations of impurities located in the bulk plasma. A detailed description of the design and the performance of both spectrometers can be found in Ref.[10].

III. GLOBAL IMPURITY TRANSPORT AT W7-X

This section discusses global transport properties of W7-X based on measurements of impurity transport

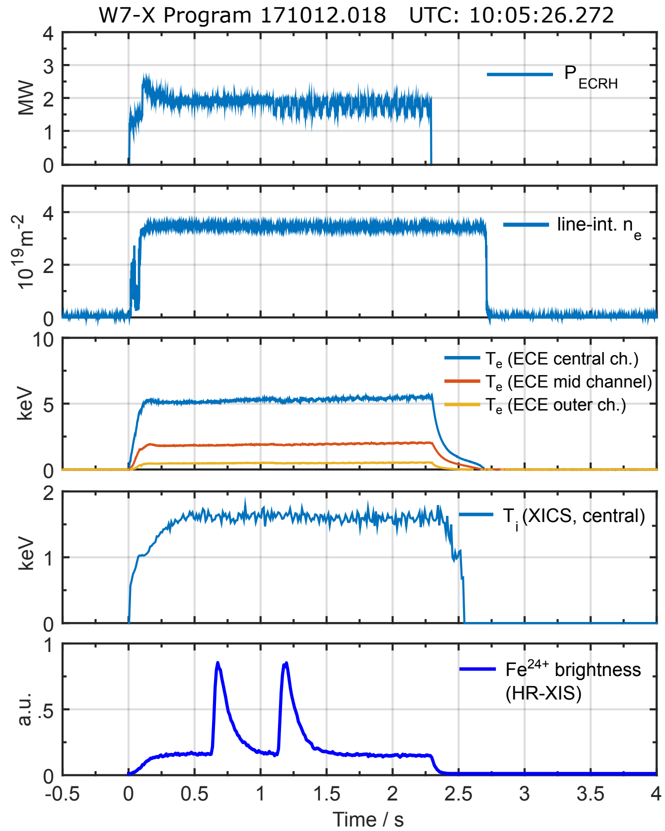

FIG. 1. Time traces of a centrally ECR heated experiment program showing the total ECR heating power P_{ECRH}, line of sight integrated density n_e, central, mid, and outer radius electron temperatures, central ion temperature, and the brightness of He-like iron emission lines.

times τ_i and energy confinement times τ_E within a systematic scan of the electron density n_e and the electron cyclotron resonance (ECR) heating power P_{ECRH}. It should be mentioned that the purity of the investigated He plasmas is to some extend reduced, with usual H gas concentrations between 5-30 % as evident from measurements of the edge He and H densities, possibly affecting the here discussed absolute values of τ_I and τ_E.

A. Measurement of Impurity Transport Times

As reported in previous works[10,11], the measurement of the exponential decay of the impurity signal after a pulsed impurity injection allows to determine the impurity transport time τ_I that is closely related to impurity transport properties. According to Ref.[10], τ_I is defined as the time constant of the exponential decaying impurity signal after achieving an ionization equilibrium[10,11]. Since the obtained impurity signal varies with T_e and n_e, the impurity injection is realized within the flat top phase of an experiment when T_e and n_e profiles are stationary. Fig.1 shows typical time traces of a centrally ECR heated experiment program with Fe injections, showing the total heating power P_{ECRH}, the line of sight integrated electron density n_e measured by the interferometer, the central T_e and T_i values as measured by the electron cyclotron emission and XICS diagnostics, and the Fe^{24+} line brightness observed with the HR-XIS spectrometer. The two distinct peaks in the Fe^{24+} signal at $t = 0.7$ s and $t = 1.2$ s originate from two single Fe injections via the LBO system, showing the above mentioned exponential decay of the Fe^{24+} signal. Here, two iron pulses have been injected to check for a possible impurity accumulation that however could not be observed in any of the performed experiment programs, even for multiple Fe injections. The background signal level before and after the Fe injections is induced by the Bremsstrahlung background radiation. The shown time traces demonstrate stationary plasma conditions for $t \geq 0.5$ s and also the non perturbing character of the injected Fe tracer impurity.

B. Impurity Transport Time Scaling

The empirical scaling of τ_I with respect to P_{ECRH} and n_e has been investigated in the magnetic standard configuration EIM and the magnetic high mirror configuration KJM of W7-X[21] by performing several experiment programs similar to that shown in Fig.1. Therefore, P_{ECRH} and n_e have been scanned systematically from the lowest possible values up to the maximum available heating power and the appearance of a density limit, terminating the experiment program by a radiation collapse[24]. All programs have been performed with the working gas helium.

The obtained τ_I values are shown in color code in Fig.2 for each experiment program with the corresponding P_{ECRH} and n_e parameters. In both magnetic configurations, two clear trends can be observed. On the one hand, τ_I decreases with increasing P_{ECRH}, being well known in literature as power degradation[25–27]. Here, the increased heating power leads to a reduced confinement of impurity species. On the other hand, τ_I increases with increasing n_e. This enhanced confinement of impurities towards higher n_e has also been observed in many other machines.

For a quantitative assessment of these effects, the scaling of τ_I with P_{ECRH} and n_e has been fitted to a two dimensional function according to the typical scaling[28]

$$\tau_I \propto \gamma \cdot P_{\text{ECRH}}^{\alpha} \cdot n_e^{\beta} \qquad (1)$$

with the free parameters α, β, and γ. For visualization, the 2D surfaces resulting from the data fit are shown together with the discrete τ_I values in the top of Fig.3 for the EIM and KJM configurations on identical scales, respectively. As already evident from the figure, the scaling of τ_I with P_{ECRH} and n_e is very similar for both magnetic configurations. In fact, the determined values for the fit parameters γ, α, and β are identical for the EIM and the KJM configuration within the experimental uncertainties as listed in Tab.I. The bottom of Fig.3 compares measured τ_I values to predicted ones τ_I^{REG} according to the scaling law (Eq.1), yielding coefficients of determination (CoD) of 0.66 and 0.75 for the EIM and KJM configurations, respectively.

τ_I scaling parameters	EIM	KJM
α	-0.49 ± 0.07	-0.60 ± 0.06
β	0.19 ± 0.03	0.21 ± 0.03
γ	140 ± 10	130 ± 8
CoD	0.66	0.75

TABLE I. Fitted scaling parameters α, β, and γ according to Eq.1 for the scaling of τ_I with P_{ECRH} and n_e in He plasmas. Also given is the coefficient of determination, CoD.

C. Energy Confinement Time Scaling

In analogy to the impurity transport time, also the energy confinement time τ_E is expected to scale according to Eq.1[6]. For a direct comparison of the τ_E and τ_I scaling, τ_E has been determined for the experiment programs of the $P_{\text{ECRH}} - n_e$ scans discussed in section III B for both magnetic configurations EIM and KJM. The τ_E values have been evaluated using the diamagnetic plasma energy W_{dia} as measured by the diamagnetic loop diagnostic[29] and the total heating power P_{ECRH}:

$$\tau_E = W_{\text{dia}} / \left(P_{\text{ECRH}} - dW_{\text{dia}}/dt\right). \qquad (2)$$

To improve statistics, here τ_E has been evaluated at several time points within the experiment programs, providing more data points for the P_{ECRH} - n_e scan compared to the impurity transport times evaluated only at times of impurities injected with the LBO.

The resulting τ_E values show a pronounced scaling with P_{ECRH} and n_e, very similar to that obtained for τ_I, including the effects of power degradation with increasing P_{ECRH} and improved confinement with increasing n_e[30]. A quantitative analysis (compare section III B) yields the scaling parameters listed in Tab.II. The α, β, and γ values given here compare well to values derived from a more general τ_E scaling study, including all experiment programs from the last W7-X experimental campaign[30]. Fig.4 compares calculated energy confinement times τ_E^{REG} using scaling parameters given in Tab.II to actual measured ones, τ_E, with the solid line corresponding to τ_E^{REG}=τ_E. For both configurations, EIM and KJM, the scaling of τ_E is well described with CoD values of 0.87 and 0.91.

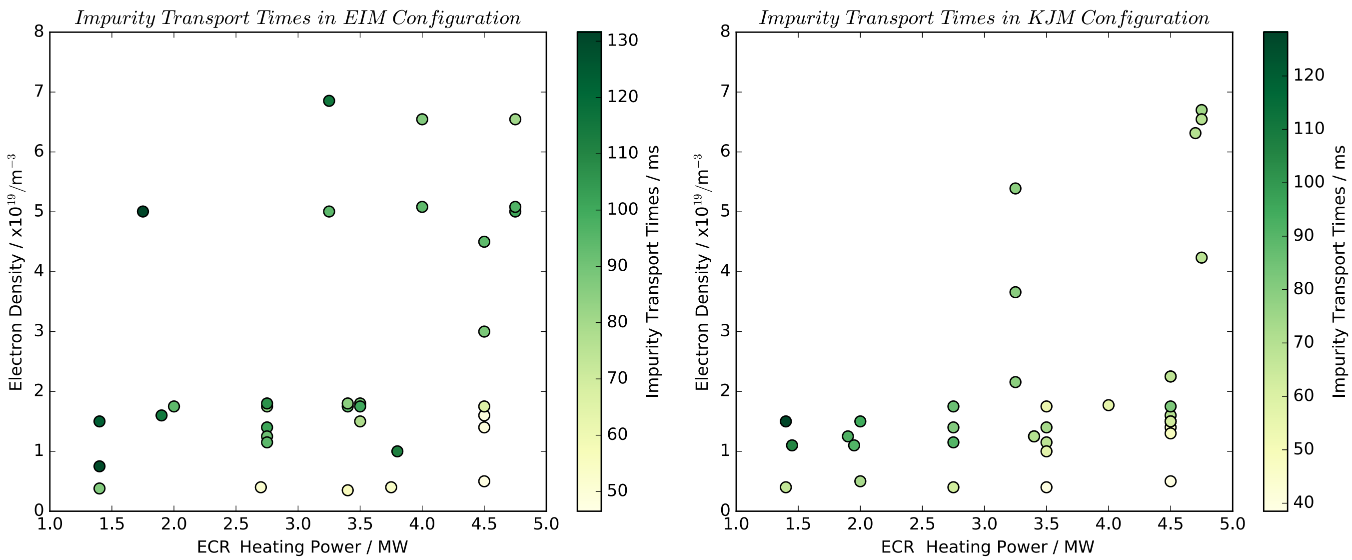

FIG. 2. Scaling of τ_I with respect to P_{ECRH} and n_e in the magnetic configurations EIM (left) and KJM (right).

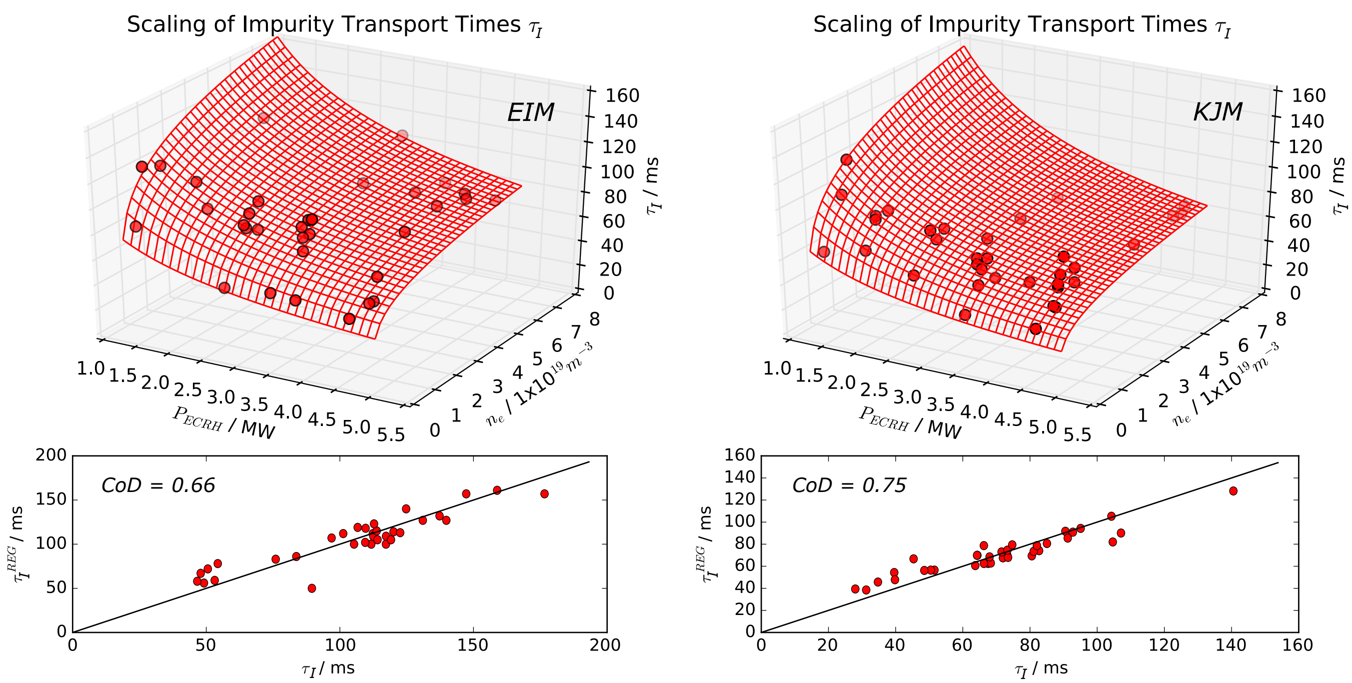

FIG. 3. Top: Fitted τ_I scaling (meshgrid) from a two dimensional least squares fit of discrete τ_I values (dots) with respect to P_{ECRH} and n_e according to Eq.1. Bottom: Linear regression curve for fitted and actual measured τ_I values in the magnetic configurations EIM (left) and KJM (right).

D. Heating Power Deposition

Additionally to the P_{ECRH} and n_e scaling of the impurity transport times, another variation of τ_I has been observed when varying the ECR heating power deposition from pure on-axis to pure off-axis heating. The different heating deposition profiles have been achieved making use of the ECRH steering launcher, installed at the W7-X ECRH system[31] that allows to deposit the heating power at different radial locations inside the plasma.

For the study of the heating power deposition effect on the impurity confinement, two identical experiment programs, 171012.018 and 171012.042 have been performed, guiding the heating power of 4 gyrotrons on radial positions pure on-axis at $\rho = 0$ and off-axis at $\rho = 0.45$ with a total heating power of $P_{\mathrm{ECRH}} = 2.0$ MW. In both experiment programs, static plasma conditions have been achieved, see Fig.1, with reproducible and identical line

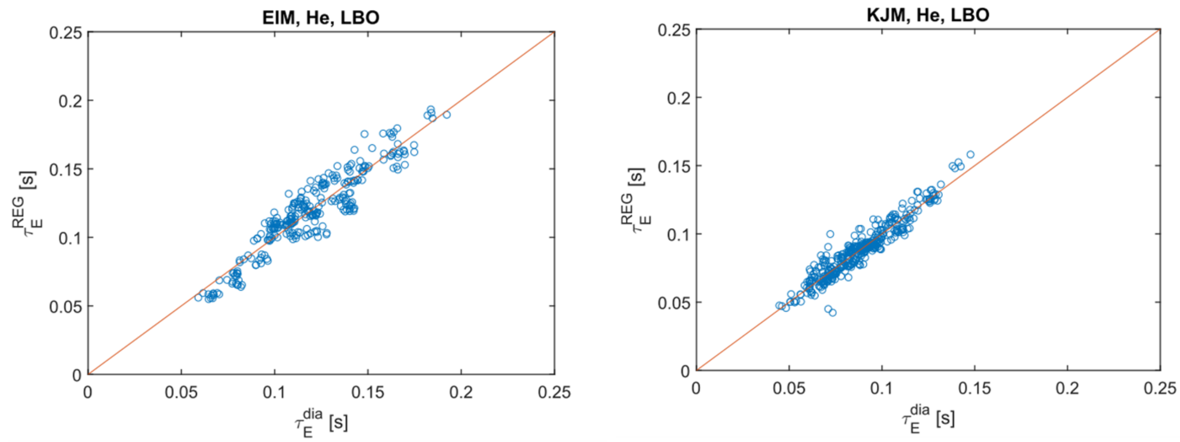

FIG. 4. Linear regression curve for fitted and actual measured τ_E values in the magnetic configurations EIM (left) and KJM (right).

τ_E scaling parameters	EIM	KJM
α	-0.64 ± 0.02	-0.60 ± 0.01
β	0.23 ± 0.01	0.25 ± 0.01
γ	188 ± 2	141 ± 1
CoD	0.87	0.91

TABLE II. Fitted scaling parameters α, β, and γ according to Eq.1 for the scaling of τ_E with P_{ECRH} and n_e in He plasmas. Also given is the coefficient of determination, CoD.

integrated electron densities and ion temperature profiles of $\langle n_e \rangle = 3.5 \times 10^{19}$ m^{-2}, and $T_i(0) = 1.7$ keV. As a consequence of the off-axis heating, the observed central T_e values are slightly reduced by 6 % with respect to central heating, resulting in also slightly reduced diamagnetic energies and energy confinement times of $W_{\mathrm{dia}} = 180$ kJ, and $\tau_E = 90$ ms for off-axis compared to $W_{\mathrm{dia}} = 190$ kJ, and $\tau_E = 95$ ms for on-axis heating.
For the impurity confinement however, a significant change in τ_I can be observed when changing from on- to off-axis heating. In fact, τ_I changes from $\tau_I = 86 \pm 1$ ms for on-axis to $\tau_I = 118 \pm 1$ ms for off-axis heating, as shown in Fig.5. Here, the left of Fig.5 shows time traces of the Fe^{24+} brightness after the Fe impurity injection for on and off-axis heating. On the right of Fig.5, a logarithmic plot of both time traces is shown together with the linear regression curves, yielding the impurity transport times given above.
A more detailed investigation, repeating the shown experiment programs with additional ECRH power deposition profiles as well as analyzing further accessible plasma parameters having impact to the impurity transport, as *e.g.* the radial electric field E_r, is ongoing and will be discussed in forthcoming publications.

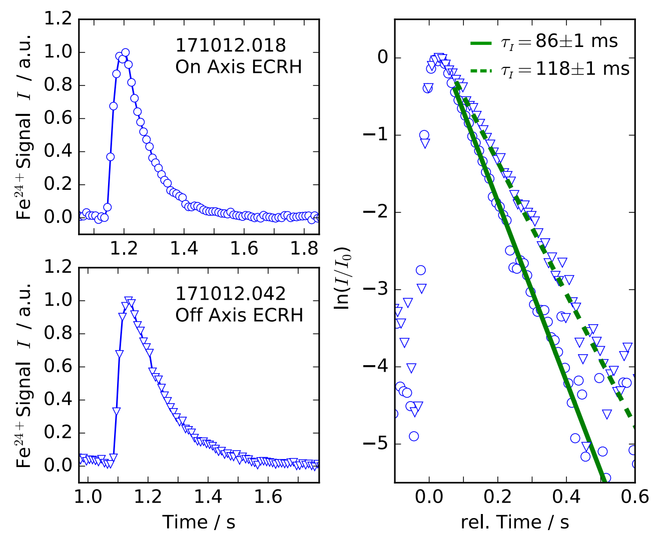

FIG. 5. Left: Time traces of Fe^{24+} line brightnesses after impurity injections for on- and off-axis ECR heating. Right: Logarithmic plot of normalized Fe^{24+} time traces and linear fits of τ_I for on-axis ECRH (solid line) and off-axis ECRH (dashed line).

IV. RESULTS AND DISCUSSION

A. Impurity and Energy Confinement

Fig.6 plots the derived scaling parameters α, β, and γ of impurity and energy confinement, see Tab.I and II, for the magnetic configurations EIM and KJM.
Comparing both magnetic configurations, the global impurity confinement turns out to be nearly identical, as demonstrated by the scaling parameters α, β, and γ matching each other within the uncertainties, see Fig.6, triangles. The same is true for the scaling of the en-

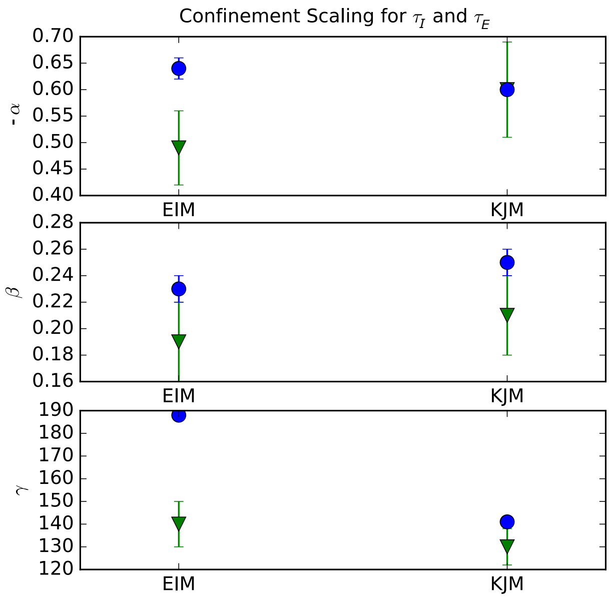

FIG. 6. Overview on the scaling parameters α, β, and γ for the τ_I (triangles) and τ_E scaling (circles) in the EIM and KJM configurations.

ergy confinement with respect to P_{ECRH} and n_e, yielding within the uncertainties nearly equal values for α and β, see circles in Fig.6. However, the absolute τ_E values are on average slightly enhanced for the EIM configuration, as evident from $\gamma(EIM) > \gamma(KJM)$, see circles in the bottom of Fig.6.

A comparison of the energy and impurity confinement shows a slightly improved energy confinement in both configurations, as reflected by the generally increased scaling parameters: $\{\alpha, \beta, \gamma\}(\tau_E) > \{\alpha, \beta, \gamma\}(\tau_I)$. This enhanced energy confinement over impurity confinement for high Z materials has also been observed for the low confinement regimes at the Tokamaks JET and Tore Supra[6].

Results from neoclassical calculations including measured T_e, T_i, and n_e profiles[25,30] shows that neoclassical theory alone can not reproduce the experimental findings without taking into account turbulent transport. In particular, the experimentally obtained τ_E values are significantly lower than those derived from neoclassical theory, roughly in the order of 50 %[30]. A similar trend can be observed also for the impurity transport: While from neoclassical theory, the predicted diffusive transport coefficient profile $D(\rho)$ is constant along ρ with an absolute value of $D < 0.1$ m^2/s[32], the actual measured profile of $D(\rho)$ significantly rises towards the plasma edge with peaking values of $D \leq 1.5$ m^2/s as derived from recent Fe impurity transport and earlier Ar impurity transport studies at W7-X[12,32]. Both observations suggest significant turbulent contributions to the energy as well as the impurity transport within the machine parameters, W7-X has been operated so far.

B. Heating Power Deposition

In large scale fusion devices, impurities can be prevented from accumulating inside the plasma center by applying a strong central ECR heating. This pretty robust effect is known as central impurity pump out and has been observed in several experiments[5,33]. Hence, the increased τ_I value for the off-axis ECR heating observed in this study is most probably related to the lack of the impurity pump out, possibly accompanied by a change in the radial electric field E_r when the ECR heating power is not focused into the plasma center. As mentioned above, for a more detailed investigation of this effect, further experimental programs are going to be conducted in the upcoming experimental campaigns of W7-X.

V. SUMMARY

In this work the impurity and energy confinement scaling of purely ECR heated plasmas has been investigated in two different magnetic configurations of W7-X. In terms of impurity transport, both configurations are indistinguishable from each other while the energy confinement in the EIM configuration is enhanced by 30 % with respect to the KJM configuration. On average, the energy confinement is slightly enhanced over the impurity confinement ($\tau_E/\tau_I = 1.3$) with observed absolute values of τ_I=40-130 ms and τ_E=40-190 ms. A change in the ECR heating power deposition profile induces a significant change in the impurity confinement, most probably related to the well known enhanced impurity pump out induced by central ECR heating[5,33].

VI. ACKNOWLEDGMENTS

This work has been carried out within the framework of the EUROfusion Consortium and has received funding from the Euratom research and training programme 2014-2018 under grant agreement No 633053. The views and opinions expressed herein do not necessarily reflect those of the European Commission.

[1] J. Garcia-Regana, C. Beidler, R. Kleiber, P. Helander, A. Mollen, J. Alonso, M. Landreman, H. Maaßberg, H. Smith, Y. Turkin, and J. Velasco, Nuclear Fusion **57**, 056004 (2017).
[2] P. Helander, S. L. Newton, A. Mollén, and H. M. Smith, Phys. Rev. Lett. **118**, 155002 (2017).
[3] E. Scavino, J. Bakos, H. Weisen, and T. Team, Plasma Physics and Controlled Fusion **46**, 857 (2004).
[4] Y. Nakamura, Y. Takeiri, R. Kumazawa, M. Osakabe, T. Seki, B. Peterson, K. Ida, H. Funaba, M. Yokoyama, N. Tamura, A. Komori, S. Morita, K. Sato, K. Narihara, S. Inagaki, T. Tokuzawa, S. Masuzaki, J. Miyazawa, N. Noda, T. Mutoh,

T. Shimozuma, K. Kawahata, Y. Oka, H. Suzuki, N. Ohyabu, T. Akiyama, N. Ashikawa, M. Emoto, P. Goncharov, M. Goto, H. Idei, K. Ikeda, S. Imagawa, M. Isobe, O. Kaneko, H. Kawazome, K. Khlopenkov, T. Kobuchi, A. Kostrioukov, S. Kubo, Y. Liang, T. Minami, T. Morisaki, S. Murakami, S. Muto, K. Nagaoka, Y. Nagayama, H. Nakanishi, Y. Narushima, K. Nishimura, T. Notake, H. Nozato, S. Ohdachi, S. Okamura, T. Ozaki, A. Sagara, T. Saida, K. Saito, S. Sakakibara, R. Sakamoto, M. Sasao, M. Sato, M. Shoji, N. Takeuchi, K. Tanaka, M. Tanaka, K. Toi, Y. Torii, K. Tsumori, K. Watanabe, T. Watari, Y. Xu, H. Yamada, I. Yamada, S. Yamamoto, T. Yamamoto, S. Yoshimura, Y. Yoshimura, M. Yoshinuma, K. Itoh, T. Mito, K. Ohkubo, I. Ohtake, T. Satow, S. Sudo, T. Uda, K. Yamazaki, K. Matsuoka, O. Motojima, Y. Hamada, and M. Fujiwara, Nuclear Fusion **43**, 219 (2003).

[5] R. Dux, R. Neu, A. G. Peeters, G. Pereverzev, A. Mück, F. Ryter, J. Stober, and A. U. Team, Plasma Physics and Controlled Fusion **45**, 1815 (2003).

[6] M. Mattioli, R. Giannella, R. Myrnas, C. Demichelis, B. Denne-Hinnov, T. D. D. Wit, and G. Magyar, Nuclear Fusion **35**, 1115 (1995).

[7] E. S. Marmar, J. E. Rice, and S. L. Allen, Phys. Rev. Lett. **45**, 2025 (1980).

[8] Y. Nakamura, N. Tamura, M. Yoshinuma, C. Suzuki, S. Yoshimura, M. Kobayashi, M. Yokoyama, M. Nunami, M. Nakata, K. Nagaoka, K. Tanaka, B. Peterson, K. Ida, M. Osakabe, T. Morisaki, and the LHD Experiment Group, Nuclear Fusion **57**, 056003 (2017).

[9] Y. Nakamura, M. Kobayashi, S. Yoshimura, N. Tamura, M. Yoshinuma, K. Tanaka, C. Suzuki, B. J. Peterson, R. Sakamoto, T. Morisaki, and the LHD Experiment Group, Plasma Physics and Controlled Fusion **56**, 075014 (2014).

[10] A. Langenberg, N. Pablant, T. Wegner, P. Traverso, A. Marchuk, T. Bräuer, B. Geiger, G. Fuchert, S. Bozhenkov, E. Pasch, O. Grulke, F. Kunkel, C. Killer, D. Nicolai, G. Satheeswaran, K. Hollfeld, B. Schweer, T. Krings, P. Drews, G. Offermanns, A. Pavone, J. Svensson, A. Alonso, R. Burhenn, R. Wolf, and the W7-X Team, "Prospects of x-ray imaging spectrometers for impurity transport: Recent results from the stellarator wendelstein 7-x," Submitted for publication to Review of Scientific Instruments.

[11] T. Wegner, B. Geiger, F. Kunkel, R. Burhenn, T. Schröder, C. Biedermann, B. Buttenschön, G. Cseh, P. Drews, O. Grulke, K. Hollfeld, C. Killer, G. Kocsis, T. Krings, A. Langenberg, O. Marchuk, U. Neuner, D. Nicolai, G. Offermanns, N. Pablant, K. Rahbarnia, G. Satheeswaran, J. Schilling, B. Schweer, T. Szepesi, H. Thomsen, and the W7-X Team, "Design, capabilities and first results of the new laser blow-off system on wendelstein 7-x," Accepted for publication in Review of Scientific Instruments.

[12] A. Langenberg, N. Pablant, O. Marchuk, D. Zhang, J. Alonso, R. Burhenn, J. Svensson, P. Valson, D. Gates, M. Beurskens, R. Wolf, and the W7-X Team, Nuclear Fusion **57**, 086013 (2017).

[13] K. Zhang, Z.-Y. Cui, P. Sun, C.-F. Dong, W. Deng, Y.-B. Dong, S.-D. Song, M. Jiang, Y.-G. Li, P. Lu, and Q.-W. Yang, Chinese Physics B **25**, 065202 (2016).

[14] J. Arevalo, J. A. Alonso, K. J. McCarthy, and J. L. Velasco, Nuclear Fusion **53**, 023003 (2013).

[15] S. Menmuir, L. Carraro, A. Alfier, F. Bonomo, A. Fassina, G. Spizzo, and N. Vianello, Plasma Physics and Controlled Fusion **52**, 095001 (2010).

[16] M. Leigheb, M. Romanelli, L. Gabellieri, L. Carraro, M. Mattioli, C. Mazzotta, M. E. Puiatti, L. Lauro-Taroni, M. Marinucci, S. Nowak, L. Panaccione, V. Pericoli, P. Smeulders, O. Tudisco, C. Sozzi, M. Valisa, and the FTU team, Plasma Physics and Controlled Fusion **49**, 1897 (2007).

[17] O. Marchuk, M. Z. Tokar, G. Bertschinger, A. Urnov, H. . J. Kunze, D. Pilipenko, X. Loozen, D. Kalupin, D. Reiter, A. Pospieszczyk, W. Biel, M. Goto, and F. Goryaev, Plasma Physics and Controlled Fusion **48**, 1633 (2006).

[18] R. Burhenn, J. Baldzuhn, R. Brakel, H. Ehmler, L. Giannone, P. E. Grigull, J. Knauer, M. Krychowiak, M. Hirsch, K. Ida, H. Maassberg, G. K. McCormick, E. Pasch, H. Thomsen, A. Wel, W.-A. Team, E. Group, and N. Group, Fusion Science and Technology **46**, 115 (2004), https://doi.org/10.13182/FST04-A547.

[19] N. A. Pablant, A. Langenberg, A. Alonso, C. D. Beidler, M. Bitter, S. Bozhenkov, R. Burhenn, M. Beurskens, L. Delgado-Aparicio, A. Dinklage, G. Fuchert, D. Gates, J. Geiger, K. W. Hill, U. Höfel, M. Hirsch, J. Knauer, A. Krämer-Flecken, M. Landreman, S. Lazerson, H. Maaßberg, O. Marchuk, S. Massidda, G. H. Neilson, E. Pasch, S. Satake, J. Svennson, P. Traverso, Y. Turkin, P. Valson, J. L. Velasco, G. Weir, T. Windisch, R. C. Wolf, M. Yokoyama, D. Zhang, and W.-X. Team, Physics of Plasmas **25**, 022508 (2018), https://doi.org/10.1063/1.4999842.

[20] N. A. Pablant, M. Bitter, R. Burhenn, L. Delgado-Aparicio, R. Ellis, D. Gates, M. Goto, K. W. Hill, A. Langenberg, S. Lazerson, M. Mardenfeld, S. Morita, G. H. Neilson, and T. Oishi, in *41st EPS conference, ECA*, Vol. 38F (2014) p. 1.076.

[21] T. Andreeva, "Vacuum magnetic configurations of wendelstein 7-x," Tech. Rep. (Max-Planck-Institut für Plasmaphysik, Garching, 2002).

[22] A. Langenberg, J. Svensson, H. Thomsen, O. Marchuk, N. A. Pablant, R. Burhenn, and R. C. Wolf, Fusion Science and Technology **69**, 560 (2016), http://dx.doi.org/10.13182/FST15-181.

[23] J. Svensson and A. Werner, in *International Symposium on Intelligent Signal Processing-WISP* (2007) pp. 955–960.

[24] G. Fuchert, S. Bozhenkov, R. Burhenn, M. Jakubowski, H. Niemann, E. Pasch, T. S. Pedersen, D. Zhang, R. C. Wolf, T. Wendelstein, and G. A. Wurden, in *2017 European Conference on Circuit Theory and Design (ECCTD)* (2017) pp. 1–4.

[25] A. Dinklage, C. Beidler, P. Helander, G. Fuchert, H. Maassberg, K. Rahbarnia, T. Sunn Pedersen, and Y. Turkin, "Magnetic configuration effects on the wendelstein 7-x stellarator," Accepted for publication in Nature Physics.

[26] B. P. van Milligen, B. A. Carreras, C. Hidalgo, and A. Cappa, Physics of Plasmas **25**, 062503 (2018), https://doi.org/10.1063/1.5029881.

[27] H. Yamada, S. Murakami, K. Yamazaki, O. Kaneko, J. Miyazawa, R. Sakamoto, K. Watanabe, K. Narihara, K. Tanaka, S. Sakakibara, M. Osakabe, B. Peterson, S. Morita, K. Ida, S. Inagaki, S. Masuzaki, T. Morisaki, G. Rewoldt, H. Sugama, N. Nakajima, W. Cooper, T. Akiyama, N. Ashikawa, M. Emoto, H. Funaba, P. Goncharov, M. Goto, H. Idei, K. Ikeda, M. Isobe, K. Kawahata, H. Kawazome, K. Khlopenkov, T. Kobuchi, A. Komori, A. Kostrioukov, S. Kubo, R. Kumazawa, Y. Liang, T. Minami, S. Muto, T. Mutoh, Y. Nagayama, Y. Nakamura, H. Nakanishi, Y. Narushima, K. Nishimura, N. Noda, T. Notake, H. Nozato, S. Ohdachi, N. Ohyabu, Y. Oka, T. Ozaki, A. Sagara, T. Saida, K. Saito, M. Sasao, K. Sato, M. Sato, T. Seki, T. Shimozuma, M. Shoji, H. Suzuki, Y. Takeiri, N. Takeuchi, N. Tamura, K. Toi, T. Tokuzawa, Y. Torii, K. Tsumori, T. Watanabe, T. Watari, Y. Xu, I. Yamada, S. Yamamoto, T. Yamamoto, M. Yokoyama, Y. Yoshimura, M. Yoshinuma, T. Mito, K. Itoh, K. Ohkubo, I. Ohtake, T. Satow, S. Sudo, T. Uda, K. Matsuoka, and O. Motojima, Nuclear Fusion **43**, 749 (2003).

[28] R. Burhenn, Y. Feng, K. Ida, H. Maassberg, K. McCarthy, D. Kalinina, M. Kobayashi, S. Morita, Y. Nakamura, H. Nozato, S. Okamura, S. Sudo, C. Suzuki, N. Tamura, A. Weller, M. Yoshinuma, and B. Zurro, Nuclear Fusion **49**, 065005 (2009).

[29] K. Rahbarnia, H. Thomsen, U. Neuner, J. Schilling, J. Geiger, G. Fuchert, T. Andreeva, M. Endler, D. Hathiramani, T. Bluhm, M. Zilker, B. B. Carvalho, and A. Werner, Nuclear Fusion (2018).

[30] G. Fuchert, S. Bozhenkov, N. Pablant, K. Rahbarnia, Y. Turkin, A. Alonso, T. Andreeva, C. Beidler, M. Beurskens, A. Dinklage, J. Geiger, M. Hirsch, U. Höfel, J. Knauer, A. Langenberg, H. Laqua, H. Niemann, E. Pasch, T. S. Pedersen, T. Stange, J. Svennson, H. Trimino Mora, G. Wurden, D. Zhang, R. C. Wolf, and W.-X. Team, "Global energy confinement in the initial lim-

iter configuration of wendelstein 7-x," Submitted for publication.
[31]S. Marsen, Y. Corre, H. Laqua, V. Moncada, D. Moseev, H. Niemann, M. Preynas, T. Stange, and T. W.-X. Team, Nuclear Fusion **57**, 086014 (2017).
[32]B. Geiger, T. Wegner, R. Burhenn, B. Buttenschön, A. Langenberg, T. Puetterich, R. Dux, T. Windisch, G. Fuchert, N. Pablant, Y. Turkin, C. Beidler, P. Traverso, and V. Winters, "Experimental study of the impurity transport in w7-x based on laser-blow-off injections and modeling using strahl and dkes," To be published.
[33]N. Tamura, C. Suzuki, S. Satake, Y. Nakamura, M. Nunami, H. Funaba, K. Tanaka, M. Yoshinuma, K. Ida, and S. Sudo, Physics of Plasmas **24**, 056118 (2017), https://doi.org/10.1063/1.4983626.